

A $K^\pm \rightarrow \pi^\pm \nu \bar{\nu}$ experiment in an unseparated beam
I - Charged Particle Yields

Peter S. Cooper
December 27, 2003

Abstract

This note begins a series to study the design choices for a $K^\pm \rightarrow \pi^\pm \nu \bar{\nu}$ experiment performed in an unseparated beam. I evaluate here the charged particle yields as a function of primary proton and secondary beam momentum based upon the published parameterizations of the SPY/NA56 data.

1 Introduction

As we think about the feasibility of a $K^+ \rightarrow \pi^+ \nu \bar{\nu}$ experiment with an unseparated beam we must again revisit the question of the optimal kaon beam momentum.

The CKM SCRF separator limits the kaon beam momentum to not much more than the CKM design values of $p = 22 GeV/c$ and $\Delta p/p = \pm 2\%$ in order to limit the decay losses as the separator inter-station distance grows with momentum and degraded separation purity as the momentum bite grows. Two compromises are inherent to the CKM design. $\sim 70\%$ of kaons are lost to upstream decays in the relatively long beam line ($\sim 1.2\lambda_{decay}$) coupled with a $\sim 40\%$ kaon transmission thru the beam line and separator combines to a $\sim 12\%$ kaon efficiency. CKM needs to make 8 K^+ 's for each one which reaches the decay volume. These beam momentum choices lead to the requirement to veto with very high efficiency for π^0 's with momenta as low as $1 GeV/c$. This leads to an "unbalanced" photon veto design where $\sim 90\%$ of the photons hit the vacuum veto system and only $\sim 10\%$ hit the high performance CsI downstream. This design works well without unduly stressing either the availability of protons or the achieve-ability of the photon veto requirements. These limits are "targets of opportunity" in a redesign.

If the beam momentum constraints of the separation system are removed then a decay in flight experiment like CKM can be scaled up in beam momentum by lengthening the apparatus by a momentum scale factor. Apertures, coverage, decay fractions, etc. all scale correctly. Measurement resolutions in magnetic spectrometers can improve for higher momentum particles since the angular resolutions are preserved by scaling while the contribution of multiple Coulomb scattering goes as $1/p$. What does not scale in the CKM design are the velocity spectrometers (the K^+ and π^+ RICHs) which are tuned to particular particle velocities ($\beta\gamma$). CKM is designed to cover π^+ 's in the forward hemisphere in the K^+ rest frame. At a higher beam momentum there is a more backward region of π^+ in the K^+ rest frame where the π^+ in the lab still fall in the appropriate lab velocity region for the same pion RICH as designed for CKM. These π^+ 's have somewhat larger lab angles than in CKM making vertex resolution better and getting the π^+ 's further from the beam. Since the transverse momentum of the π^+ 's in the acceptance of the RICH are larger so are the transverse momenta of the photons from K_π^2 decays on the other side of the beam from the π^+ .

The most obvious potential limitation of an unseparated beam is the presence in the "UMS" of more than $10\times$ the flux K^+ from the other charged particles in the beam. An such experiment with a $30 MHz$ K^+ flux will have to track $> 300 MHz$ of charged particles. The kaon fraction of the unseparated beam is now a limiting factor. The choice of which charge beam to run is now

| | A | B | α | β | a | b | γ | δ | r_0 | r_1 |
|-----------|------|------|----------|---------|------|------|----------|-----------|-------|-------|
| π | 62.3 | 1.57 | 3.45 | 0.517 | 6.10 | | 0.153 | 0.478 | 1.05 | 2.65 |
| K | 7.74 | | 2.45 | 0.444 | 5.04 | | 0.121 | 2γ | 1.15 | -3.17 |
| p | 8.69 | 12.3 | | | 5.77 | 1.47 | | | | |
| \bar{p} | 5.20 | | 7.56 | 0.362 | 5.77 | | | | | |

Table 1: Invariant cross-section fit parameters from reference [5]

also subject to review. In crude terms the K^- yield per proton is half that of K^+ while the kaon fraction of the negative beam is twice that of the positive beam due to the absence of secondary protons.

There are several steps in redesigning CKM for a higher momentum, wideband beam. The first of these is to reliably estimate the yields of K^+ 's and K^- 's along with the other charge species in the beam. This is the subject of this note. The redesign and simulation of the apparatus for such an experiment is another major topic which will be the topic of subsequent notes in this series.

2 Invariant Cross-section Calculation

The NA20 [1] and NA56/SPY [2, 3, 4] experiments at CERN published secondary particle invariant production cross-sections from $400\text{GeV}/c$ and $450\text{GeV}/c$ protons incident on a Beryllium target of different lengths as a function of charged particle species, total and transverse momentum. These data were fit to parametric forms in a subsequent paper [5] as a function of a ‘‘radial’’ scaling variable; x_R defined in reference [6], and p_T .

I have translated those fits into a set of PAW kumacs to evaluate the invariant cross-section and particle yields for arbitrary proton beam momenta, production P_T and target length. The relevant formulae from reference [5] are:

$$Ed^3\sigma/dp^3[\pi^+, K^+] = A(1 - x_R)^\alpha(1 + Bx_R)x_R^{-\beta}(1 + a/x_R^\gamma P_T + a^2/x_R^\delta P_T^2)e^{-a/x_R^\gamma P_T} \quad (1)$$

$$r(\pi)[\pi^-/\pi^+] = r_0(1 + x_R)^{r_1} \quad (2)$$

$$r(K)[K^-/K^+] = r_0(1 - x_R)^{r_1} \quad (3)$$

$$Ed^3\sigma/dp^3[p] = A(1 + Bx_R)(1 - x_R)^{-bP_T^2}(1 + aP_T + a^2/2P_T^2)e^{-aP_T} \quad (4)$$

$$Ed^3\sigma/dp^3[\bar{p}] = A(1 - x_R)^\alpha x_R^{-\beta}(1 + aP_T + a^2/2P_T^2)e^{-aP_T} \quad (5)$$

Table 1, taken from reference [5], are the fit parameters used in evaluating these formulae.

3 Yield Calculation

The yield of secondary particles per proton incident on a Be target is related to the invariant cross-section by:

$$d^2N/d\Delta p d\Omega = Y = [Ed^3\sigma/dp^3][p^2/E][N_0\rho\lambda_p/A]F(L) \quad (6)$$

Where $F(L)$ is the probability that a proton interacts in a target of length L and the produced secondary particle escapes the target without under-going another interaction. For the purposes of this work I am ignoring tertiary production. This under-estimates the total yields by $\sim 10 - 30\%$ for a 40cm Be target depending upon particle type and kinematics. See reference [5] for more details.

$$F(L) = \lambda_s / (\lambda_s - \lambda_p) [1 - e^{-L(1/\lambda_p - 1/\lambda_s)}] \quad (7)$$

Values for $F(L)$ are shown for an $L = 40\text{cm}$ Be target in table 2

| s | σ_{tot}^{sp} [mb] | λ_s [cm] | $F(L)$ |
|---------|-----------------------------|---------------------|--------|
| π^+ | 23.4 | 73.2 | 0.368 |
| K^+ | 17.5 | 97.9 | 0.461 |
| p | 42.1 | 40.7 | 0.497 |

Table 2: Single interaction target efficiencies for a 40cm Be target.

Where λ_p and λ_s are the proton and secondary particle interaction lengths in Be.

4 Yield Results

I have evaluated equation 6 using all the other equations and parameters given in sections 2 and 3 above. The results are plotted in figures 1- 4. In each of these figures the upper plot is the flux of particles in $[MHz]$ assuming 4×10^{12} protons per second incident on a one interaction length (40[cm]) Beryllium target, a $1[\mu sr]$ solid angle beam at a momentum bite of $1[GeV/c]$. These yields are plotted in $1[GeV/c]$ secondary momentum bins. The lower plot in each figure is the integral of the upper plots from zero; the total rate of particles produced below the momentum p . In all cases the pion flux has been scaled down on these plots by a factor of 10 and the proton flux by a factor of 20. Anti-protons and kaons fluxes are not scaled.

Section 5 below has example on how to use these figures.

Figures 1 and 2 are the positive and negative particle yields for a Main Injector proton beam energy of $120[GeV/c]$. Figures 3 and 4 are the positive and negative particle yields for an SPS proton beam energy of $450[GeV/c]$. In figure 6 I plot the K^+ and K^- yield ratios comparing $450[GeV/c]$ and $120[GeV/c]$ production. I've included a factor of 5 for the relative spill durations of the SPS (15[sec]) and Main Injector (3[sec]) so this plot is the ratio of kaon yield available per hour. Each machine has a similar spill duty factor of $\sim 30\%$.

5 Reality Checks

A few cross-checks are in order to verify these calculations. I've checked the evaluation of the invariant cross-sections given by equations 1- 5 by comparing to the invariant cross-section measurement tabulated in Table 1 of reference [5].

To check the yield calculation and plotting I can try to reconstruct the proposed CKM rate from data of figure 1. Reading off from this figure the yield of $22 \pm 0.5[GeV/c^2] K^+$ as $2.20[MHz]$ and referring to the CKM proposal for the CKM beam parameters yields a K^+ rate in the decay volume in unreasonably good agreement with the CKM Proposal which assumed a proton flux of

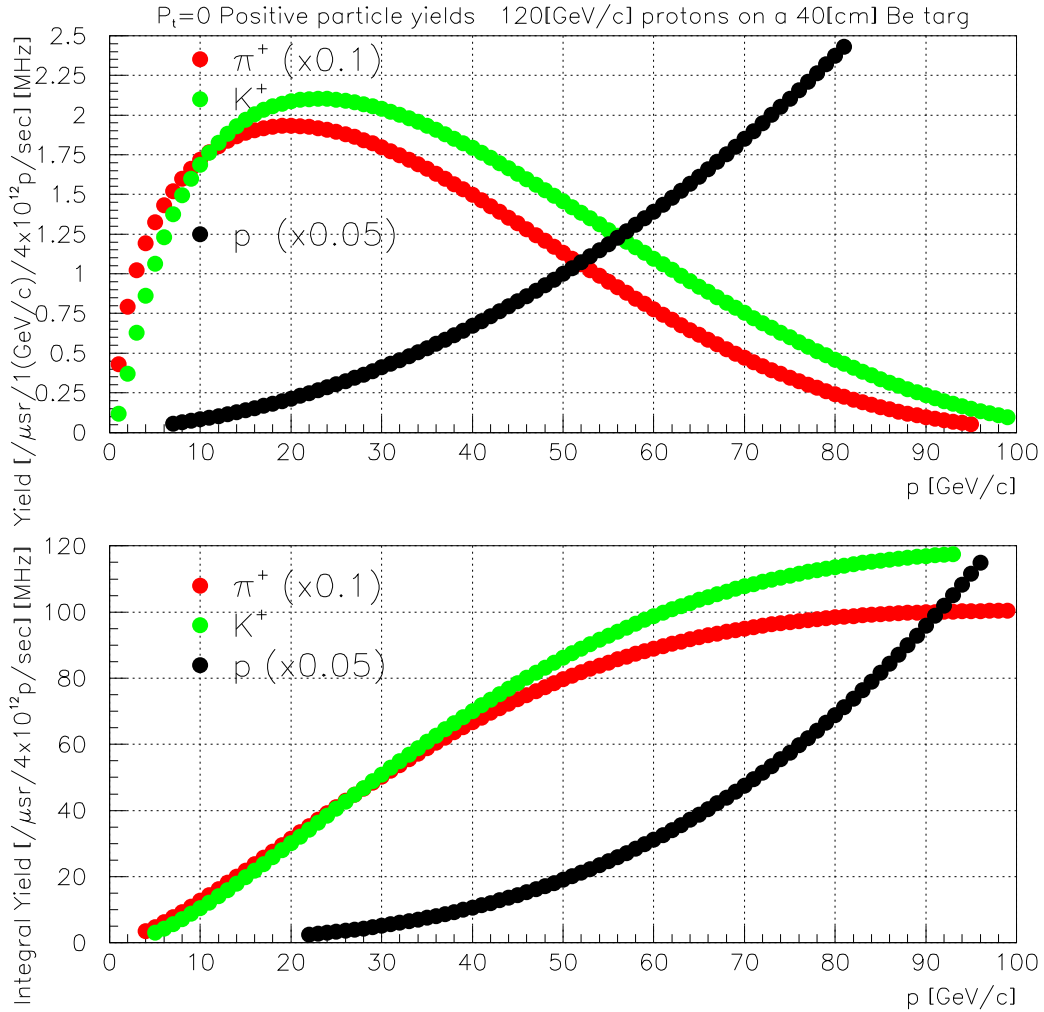


Figure 1: Forward positive particle yields from 120[GeV/c] protons on a 40[cm] Be target. Units are particles in [MHz] per 4×10^{12} protons per second per μsr per [GeV/c] momentum bite. Upper panel is the yield in 1[GeV/c] bins; the lower panel is the integral yield.

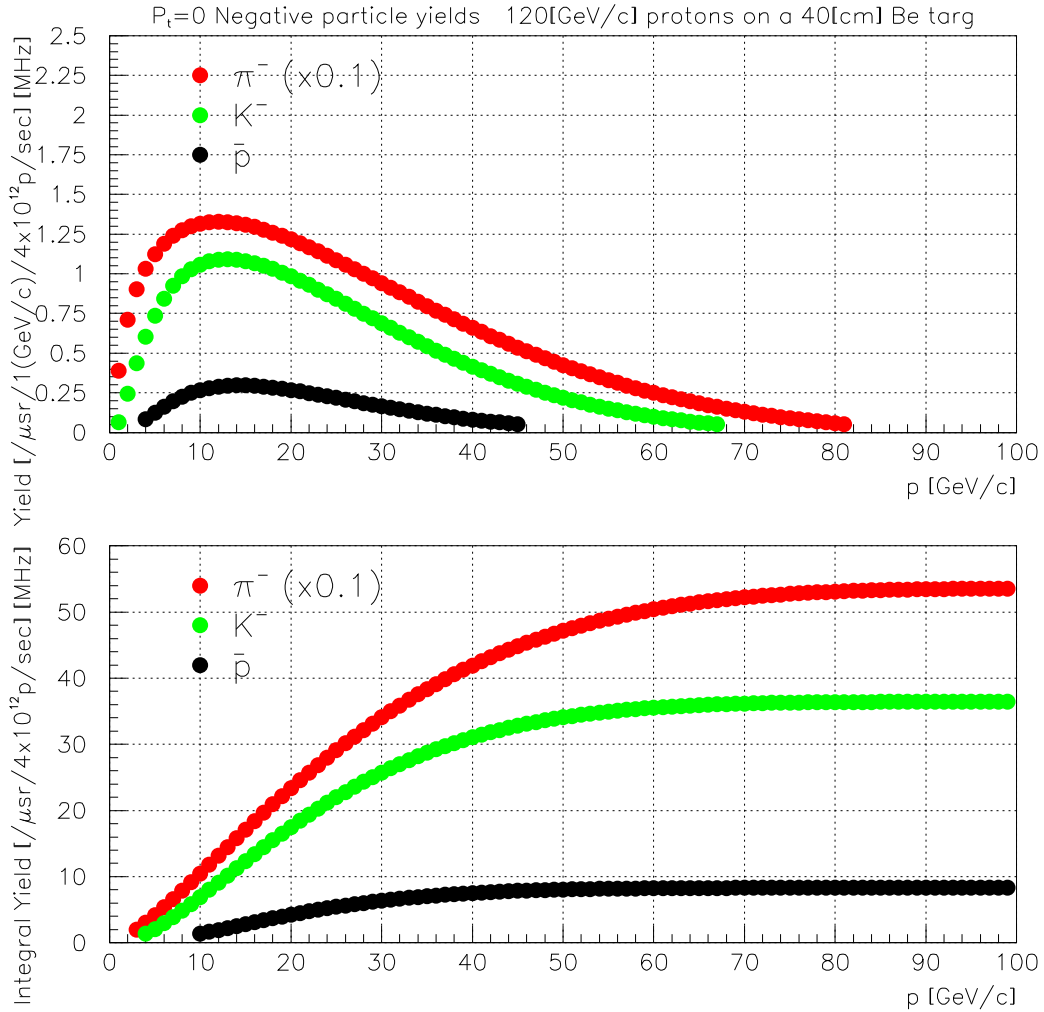


Figure 2: Forward negative particle yields from 120[GeV/c] protons on a 40[cm] Be target. Units are particles in [MHz] per 4×10^{12} protons per second per μsr per [GeV/c] momentum bite. Upper panel is the yield in 1[GeV/c] bins; the lower panel is the integral yield.

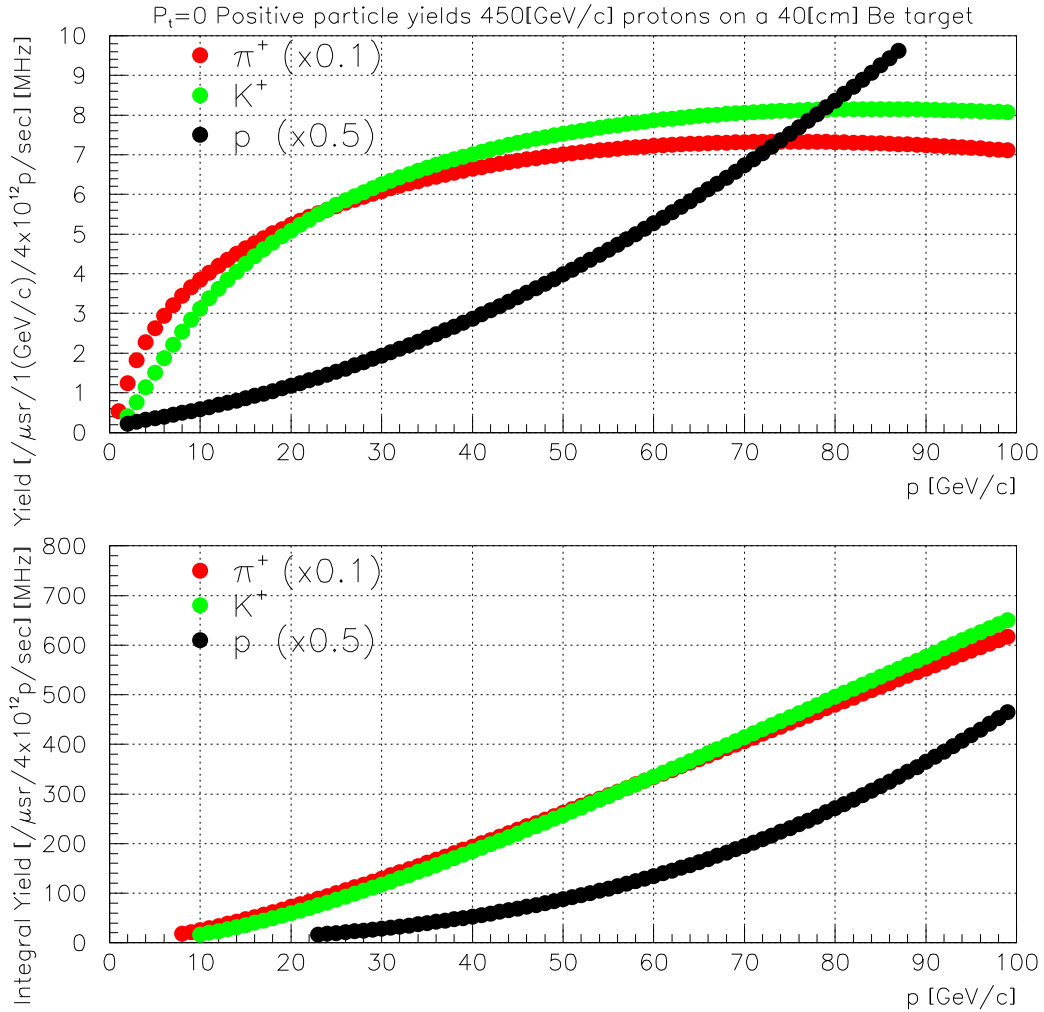


Figure 3: Forward positive particle yields from 450[GeV/c] protons on a 40[cm] Be target. Units are particles in [MHz] per 4×10^{12} protons per second per μsr per [GeV/c] momentum bite. Upper panel is the yield in 1[GeV/c] bins; the lower panel is the integral yield.

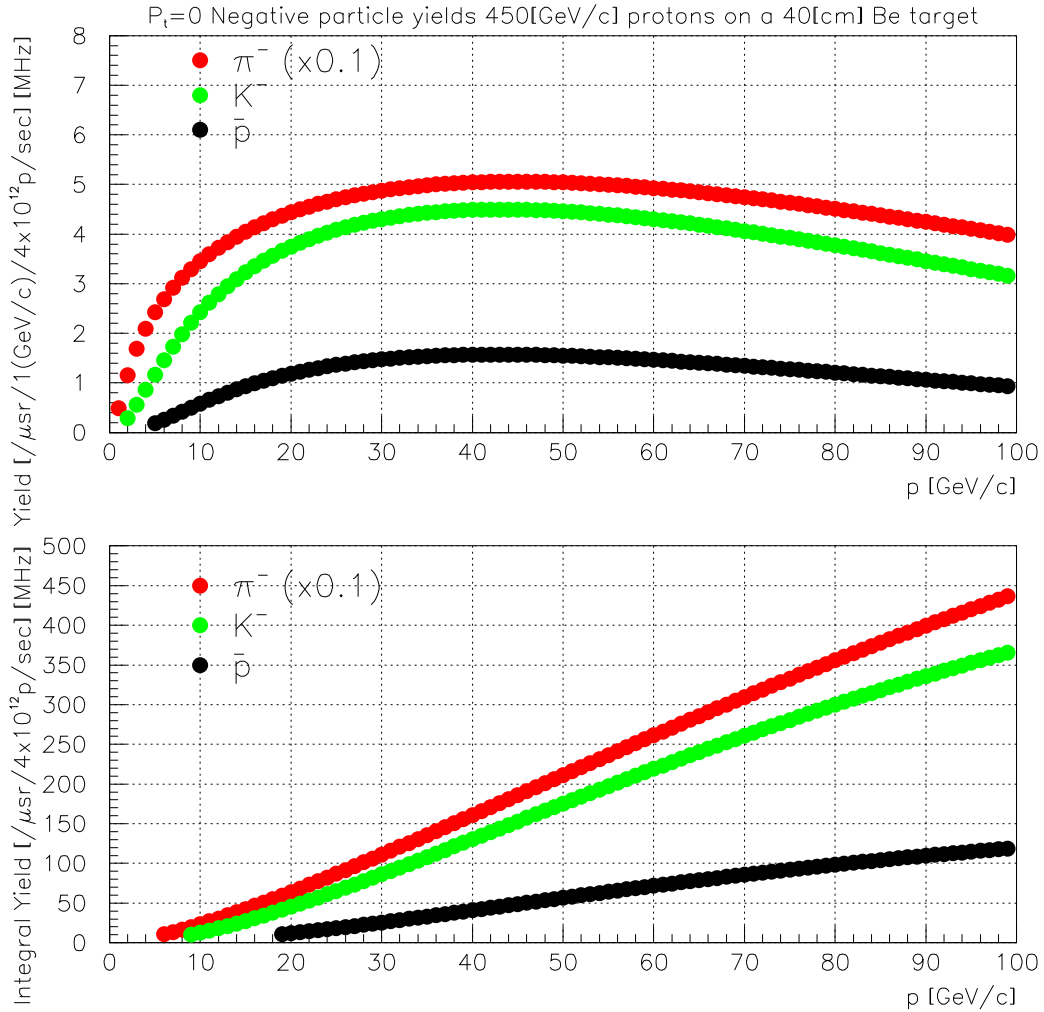


Figure 4: Forward negative particle yields from 450[GeV/c] protons on a 40[cm] Be target. Units are particles in [MHz] per 4×10^{12} protons per second per μsr per [GeV/c] momentum bite. Upper panel is the yield in 1[GeV/c] bins; the lower panel is the integral yield.

$4 \times 10^{12}[/math>sec] on a 1 interaction length Beryllium target to yield a 30[MHz] K^+ rate incident on the decay volume.$

| parameter | source | value |
|------------------------|-----------------|-------------------------------|
| Yield | Figure 1 | $2.20[MHz/\mu sr/GeV/c^2]$ |
| Proton beam | proposal | $4 \times 10^{12}[/math>sec]$ |
| Target (Be) | proposal | 40[cm] |
| Momentum bite | proposal | $\Delta p = 0.88[GeV/c]$ |
| Solid angle | proposal | $\Delta\Omega = 128[\mu sr]$ |
| K^+ produced | product | 248[MHz] |
| Decay factor | proposal (200m) | 30% |
| Separator Transmission | proposal | 40% |
| K^+ in decay volume | product | 29.5[MHz] |

Table 3: CKM rate estimate

A similar calculation for the NA48/2 beam at CERN is shown in table 4. The rate in the beam momentum interval $[57 - 63][GeV/c^2]$ is for the difference of the integral values at $57[GeV/c^2]$ and $63[GeV/c^2]$ from the lower plot of figure 3. In this case I'm reading this figures as per 4.8[sec]spill rather than per second.

The agreement here is not as good as with CKM but this is a confrontation with an actual measurement.

| parameter | source | value |
|------------------------|-----------------|---------------------------------|
| π^+ Integral Yield | Fig 3 | $430[M/spill/\mu sr]$ |
| K^+ Integral Yield | Fig 3 | $47[M/spill/\mu sr]$ |
| p Integral Yield | Fig 3 | $64[M/spill/\mu sr]$ |
| Proton flux | N.Doble's note | $1 \times 10^{12}[/math>spill]$ |
| spill length | N.Doble's note | 4.8[sec] |
| Kaon Momentum | N.Doble's note | $60[GeV/c]$ |
| Target (Be) | my memory | 30[cm] |
| correction | eqn 7 | 0.887 |
| Momentum bite | N. Doble's note | $6.0[GeV/c]$ |
| Solid angle | N. Doble's note | $0.51[\mu sr]$ |
| π^+ predicted | product | $49[M/spill]$ |
| K^+ predicted | product | $5.3[M/spill]$ |
| p predicted | product | $7.2[M/spill]$ |
| π^+ observed | N. Doble's note | $33.2[M/spill]$ |
| K^+ observed | N. Doble's note | $3.1[M/spill]$ |
| p observed | N. Doble's note | $8.6[M/spill]$ |

Table 4: NA48/2 rate estimate

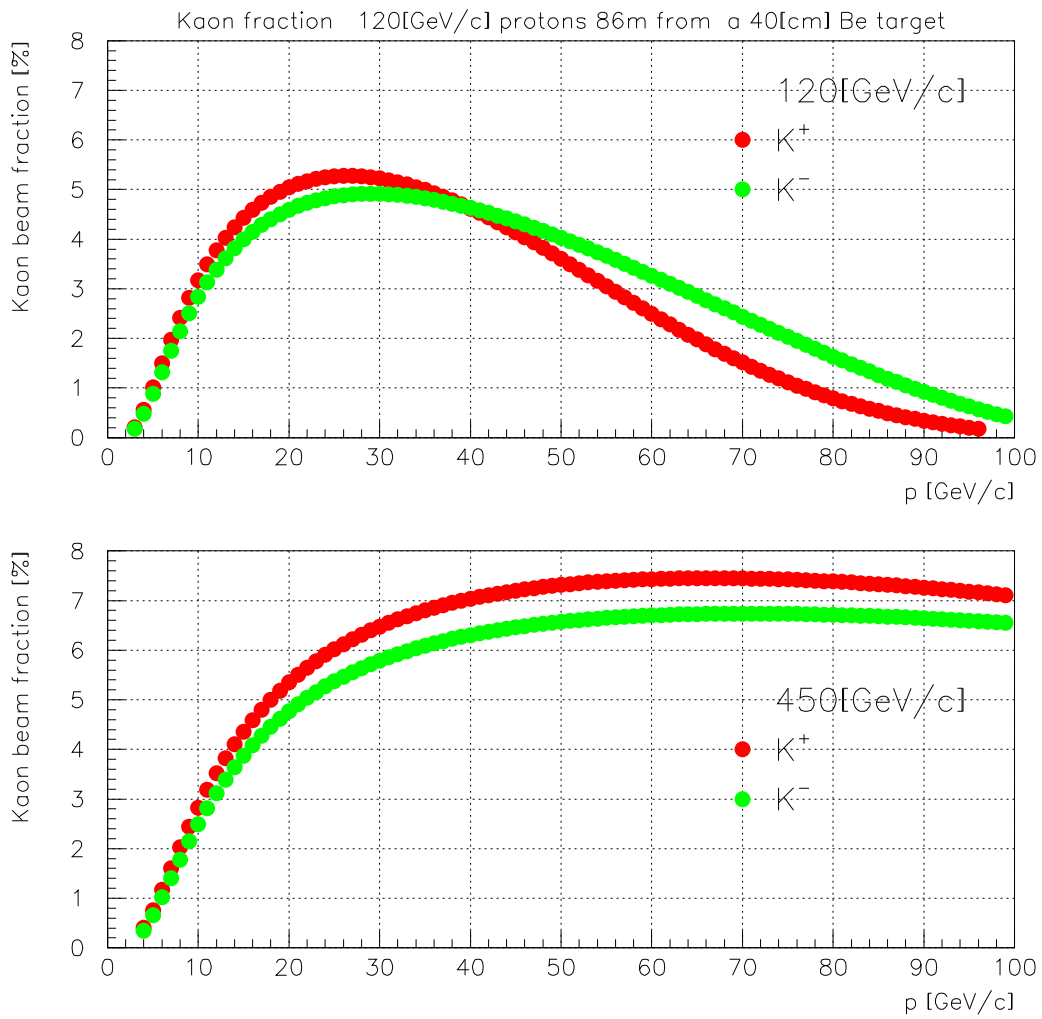


Figure 5: Kaon beam fractions for positive and negative beams at incident proton momenta of 120[GeV/c] (Main Injector) and 450[GeV/c] (SPS).

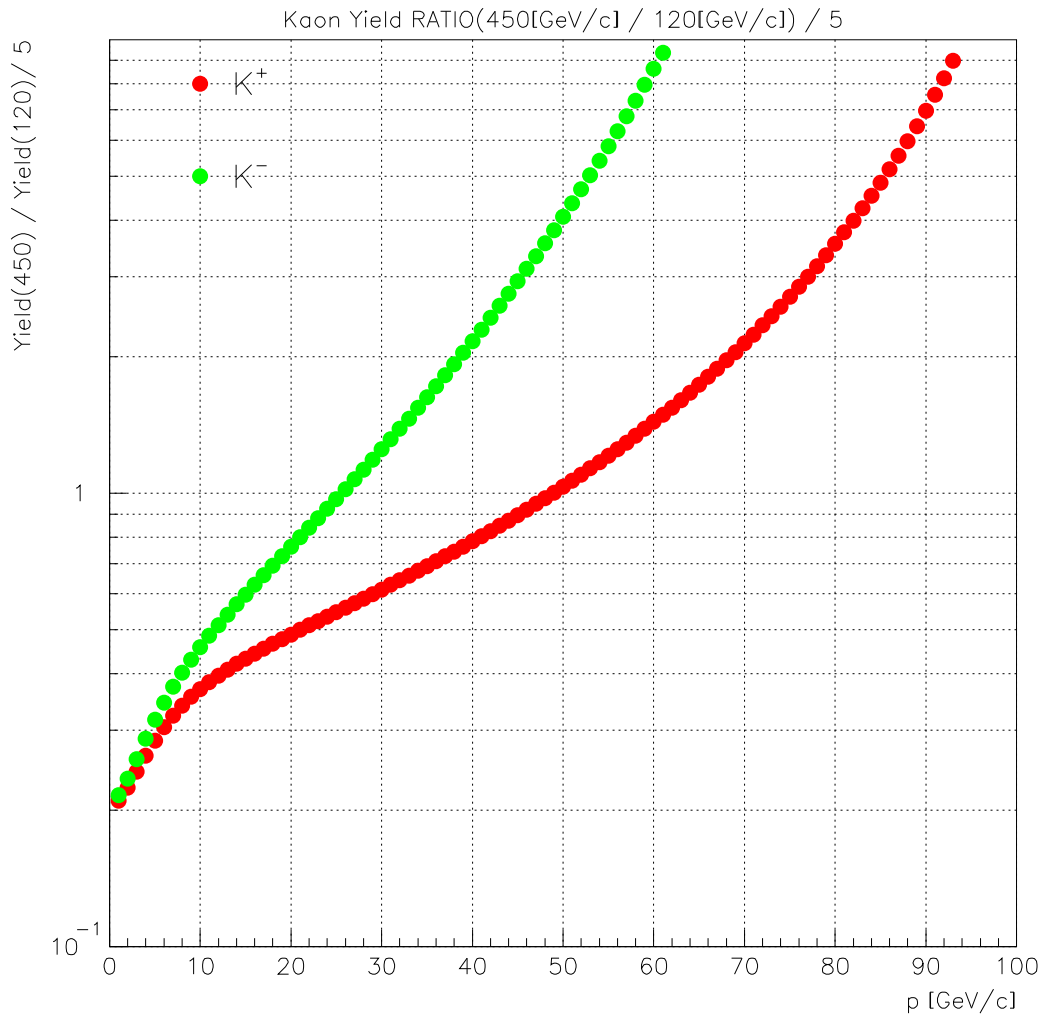


Figure 6: Ratio comparing 450[GeV/c] kaon yields at the SPS with 120[GeV/c] kaon yields at the Main Injector. A factor of 5 is included to correct for the relative cycle times of the SPS (15[sec]) and Main Injector (3[sec]).

| species Δp | rate [MHz] 30-60 | % | rate 30-55 | % | rate 30-50 | % | rate 30-45 | % | rate 37-52 | % |
|-----------------------|----------------------------|-----|---------------|-----|---------------|-----|---------------|-----|---------------|-----|
| 120GeV | 4×10^{12} p/sec | | | | | | | | | |
| p | 521 | 56. | 390 | 52. | 279 | 47. | 186 | 43. | 250. | 55. |
| π^+ | 373 | 40. | 332 | 44. | 283 | 48. | 224 | 52. | 191. | 41. |
| K^+ | 37 | 3.9 | 32 | 4.2 | 26 | 4.5 | 20 | 4.7 | 19. | 4.1 |
| π^- | 157 | 94. | 144 | 94. | 126 | 94. | 103 | 94. | 78. | 95. |
| K^- | 7.2 | 4.4 | 6.9 | 4.5 | 8.2 | 4.6 | 5.2 | 4.7 | 3.6 | 4.4 |
| \bar{p} | 1.9 | 1.1 | 1.8 | 1.2 | 1.7 | 1.3 | 1.5 | 1.3 | 0.85 | 1.0 |
| 450GeV | 4×10^{12} p/spill | | | | | | | | | |
| p | 42 | 9.0 | 32 | 8.4 | 24 | 7.9 | 16 | 7.3 | 21. | 8.8 |
| π^+ | 394 | 84. | 324 | 84. | 255 | 85 | 188 | 86. | 198. | 84. |
| K^+ | 34 | 7.2 | 27 | 7.1 | 21 | 7.0 | 15 | 6.9 | 17. | 7.2 |
| π^- | 290 | 91. | 242 | 91. | 193 | 91. | 144 | 91. | 146. | 91. |
| K^- | 21 | 6.4 | 17 | 6.4 | 13 | 6.3 | 10 | 6.2 | 10. | 6.4 |
| \bar{p} | 9.2 | 2.9 | 7.7 | 2.9 | 6.2 | 2.9 | 4.7 | 2.9 | 4.7 | 2.9 |

Table 5: Integral yields and fractions at 86m from a 40[cm] Be target production target with 4×10^{12} p/spill incident in a nominal 1[μsr] solid angle beam. This table give a direct comparison of available kaon rates at the KTeV(Fermilab-Main Injector) and NA48(Cern).

6 Yield Comparisons

The following plots and tables compare the kaon fluxes available at 86m from a 40[cm] Be target production target with 4×10^{12} p/spill incident in nominal 1[μsr] solid angle beam. These give a direct comparison of available kaon rates at the KTeV(Fermilab-Main Injector) and NA48(Cern). Table 5 shows that the available rate per beam hour are quite similar at either accelerator. The larger kaon production cross-section at low x_R in the CERN beam compensates for the factor of 5 lower cycling rate of the SPS relative to the Main-Injector. At the lower x_R value at the SPS proton production is suppressed in the positive beam. As shown in Fig 5 the K^+ beam fraction is enhanced.

7 Software

All the kumacs and other codes used for this note live in directories like ckm/beamline/ on a selection of computers including pcooper@ckm06:, pcooper@pcooper: and ckm@ckm00: and in the CKMgroup account under fsgi01: ckm/beam/beamline. The PAW kumacs and their functions are tabulated in Table 6.

References

- [1] H.W. Atherton *et.al.*, *CERN 80-07,1980*
- [2] G.Ambrosini, *et.al.*, *Phys. Lett. B420 (1998) 225.*
- [3] G.Ambrosini, *et.al.*, *Phys. Lett. B425 (1998) 208.*

| <file>.kumac | function | figure & tables |
|--------------|--------------------------------|---------------------|
| y120 | Main-Injector yields | Figure 1 - 2 |
| y450 | SPS yields | Figure 3 - 4 |
| kfrac | Kaon beam fractions | Figure 5 |
| flux-int | Flux integrals | Table 5 |
| yield | Yield[MHz] of particle species | called by flux-int |
| spy | plot invariant cross-sections | test routine |
| spy-yield | Particle yields | call by everyone |
| spyfits | Invariant cross-sections [5] | called by spy-yield |
| ratio | SPS/MI Yield ratios | Figure 6 |

Table 6: PAW kumacs used to generate the figures and tables for this note.

[4] *G.Ambrosini, et.al., Euro. Jour. Phys. C10 (1999) 605.*

[5] *M. Bonesini, et.al., Euro. Jour. Phys. C120 (2001) 13., hep-ph/0101136.*

[6] *F.E. Taylor, et.al., Phys. Rev. D14, 1217 (1976).*